



Green synthesis, Characterization and Evaluation of In-vitro Antioxidant & Anti-diabetic Activity of Nanoparticles from A Polyherbal Formulation-Mehani

J. Sasidharan, R. V. Meenakshi, P. SureshKumar*

Department of Biotechnology, Anna University, Trichy, TN, India

Received: 10.07.2018 Accepted: 14.08.2018

*drsureshbiotech2003@gmail.com



ABSTRACT

Green synthesis of silver and iron nanoparticles was carried out using Polyherbal formulation Mehani and characterized through UV-Visible absorption spectroscopy, FTIR, XRD and SEM, respectively. The colour change and strong peak at 465nm on UV-spec analysis initially conform to the synthesis of silver nanoparticles. Peaks were not obtained for iron nanoparticles since it is zero valent in nature. The FTIR study reveals the phytochemicals responsible for the reduction of silver and iron nanoparticles. The crystalline nature of the presence of silver and iron nanoparticles was confirmed by XRD analysis by comparing with standard JCPDS file No. 89-3722, 75-0033. Surface morphology and size were identified using SEM analysis, and it was found to be 60-80nm, 40-60nm, respectively. Total phenol and flavonoid content were also estimated for the synthesized nanoparticles and found to be 2.91 and 1.93 (AgNPs), 3.71 and 5.185 (FeNPs). Antioxidant activities like DPPH, Nitric oxide, H₂O₂ scavenging activities and reducing power assays were performed. The anti-diabetic activity was performed using alpha-amylase inhibition assay, and the percentage of inhibition was found to be 65.45% (AgNPs), 70.48% (FeNPs) and 73.87% for standard ascorbic acid. The result clearly indicates that FeNPs possesses better antioxidant and anti-diabetic activity that can be used for the efficient management of hyperglycemia.

Keywords: Antioxidants and diabetes; Iron nanoparticles; Poly herbal formulation; Silver.

1. INTRODUCTION

Diabetes mellitus is a chronic metabolic syndrome that occurs due to complete insulin deficiency or lesser insulin action (Dewanjee *et al.* 2009), predominantly affecting developing countries like India, China (Li *et al.* 2014) and nearly 500 million people are expected to be diabetic by the year 2025 (Liu *et al.* 2008). Both cardiovascular and obesity-related diabetic complications are increasing that is associated with free radical production (Giacco and Brownlee, 2010) and can be identified using reduced levels of antioxidant enzymes like catalase superoxide dismutase (SOD) and glutathione peroxidase (Lipinski). Owing to the unwanted side effects faced in synthetic anti-diabetic drugs, alternative herbal-based hypoglycemic drugs can be used in diabetes treatment (Patel *et al.* 2012). Studies also reveal that plants rich in polyphenols are potent antioxidant and hyperglycemic agents that can act as better radical scavengers and prevent the diabetes linked complications (Nair *et al.* 2013). Usage of the polyherbal formulation is encouraged in the traditional medicinal system due to the synergistic activity and less side effects (Kalia and Gauttam, 2013). So in this present study, green synthesis of silver and iron nanoparticles is aimed to enhance the antioxidant and anti-diabetic activity of the methanolic extract of the polyherbal formulation

Mehani using the environmentally friendly, affordable and less time-consuming technique (Balayssac *et al.* 2009).

Synthesized nanoparticles were characterized using UV-Visible spectroscopy, Fourier transforms infrared (FTIR) spectroscopy, X-ray diffraction (XRD) and Scanning electron microscopy (SEM) analysis. The presence and nature of the particle can be confirmed by performing XRD analysis. Surface morphology and size were identified by using SEM analysis.

2. MATERIALS & METHODS

2.1. Procurement of Mehani

Mehani is a polyherbal formulation containing *Tinospora cordifolia*, *Curcuma longa* *Trigonella foenum gracum* *Embllica officinale* and *Salacia oblonga*. The Polyherbal formulation was collected from K.S.Varier's Ashtanga Ayurvedics Pvt Ltd, Tiruchirappalli, Tamil Nadu, India.

2.2. Preparation of Herbal Extract

15g of mehani was extracted in 100ml of methanol for 4h in orbital shaker and filtered through No.1 whatman filter paper of 11µm pore size, dried in hot

air oven until solvent evaporates completely and stored at 4°C. The methanolic extract of mehani was allowed to react with 0.1M of AgNO₃, FeCl₃ solution separately, incubated for 4h with moderate shaking until the color change was observed. Mehani extract was used as a reducing agent or capping agent for the synthesis of silver and iron nanoparticles (Kharissova *et al.* 2013).

2.3. Characterization of Silver Nanoparticles (AgNPs) and Iron Nanoparticles (FeNPs)

2.3.1 Ultra Violet–Visible Spectroscopy

The UV–visible absorbance of the AgNPs and FeNPs was measured using UV-1800 (Shimadzu, Japan).

2.3.2 XRD Analysis

X-Ray Diffraction (XRD) analysis of drop-coated films of nanoparticles was performed for the determination of the formation of Fe and Ag nanoparticle by an X'Pert Pro X-Ray Diffractometer (X' Pert High Score Plus program) operated at a voltage of 35kV and a current of 30 mA with Cu K_{α1} radiation (Bagherzade *et al.* 2017). XRD patterns were analyzed to determine peak intensity, position, width and Full Width at Half-Maximum (FWHM). Data was used with Scherrer's formula to determine mean particle size. Scherrer's equation is: $d = 0.9\lambda / \beta \cos\theta$. Where d is the Mean diameter of the nanoparticles, λ -wavelength of the X-ray radiation source, β - angular FWHM of the XRD peak at the diffraction angle θ .

2.3.3 SEM Observation of Synthesized: Nanoparticles

The synthesized nanoparticles, after reaction, spontaneously precipitated at the bottom of the tubes and the suspension above the precipitate was sampled for SEM observation. SEM observations were carried out on a ZEISS EVO 40 EP Electron microscope.

2.4. Phytochemical Analysis

2.4.1 Determination of Total Phenol Content

To the different concentrations (50-250 µg/ml) of AgNPs and FeNPs of mehani extracts, 250µl of folin ciocalteu reagent was added. 1.5 ml of 20% Na₂CO₃ solution was added, and the final volume was made to 5ml and incubated in the dark for 2h. Total phenolic content was determined according to (McDonald *et al.* 2001) method. The absorbance was read at 760 nm. Gallic acid was used as standard. The total phenol was expressed as gallic acid equivalent (GAE/g) extract.

2.4.2 Determination of Total Flavonoid Content

Flavonoid content was determined according to (Zhishen *et al.*1999) method with some modifications.

To the different concentrations of AgNPs and FeNPs of mehani extracts, 0.3 ml of 5 % NaNO₂ and 0.3 ml of aluminium chloride (10%) was added. After 1 min, 2ml of 1M NaOH was added, and the final volume was made up to 10 ml and allowed to stand at room temperature for 30 min. Rutin was used as standard. The absorbance was read at 415nm. The amount of aluminium chloride was substituted by the same amount of distilled water in the blank. The calibration curve was plotted using standard rutin.

2.5. In Vitro Antioxidant Assay

2.5.1 DPPH Activity

The free radical scavenging activities of the plant extracts were measured employing the modified method of (Blois 1958). To the varied concentrations of AgNPs and FeNPs of mehani extracts and ascorbic acid standard (50, 100, 150,200, 250 µg/ml), 1 ml of 0.3 mM DPPH in methanol was added and incubated in the dark for 30 min. Later, the absorbance was measured at 517 nm. Control was measured containing 1 ml of methanol with DPPH without the extract. Radical scavenging activity is calculated using the formula: $((A_C - A_S)/A_C) * 100$. A_C: Absorbance of control; A_S: absorbance of the sample.

2.5.2 Hydrogen Peroxide Scavenging Assay

The hydrogen peroxide scavenging role was evaluated as per the method described by (Jayaprakasha *et al.* 2004). 2ml of 20mM hydrogen peroxide prepared in phosphate buffer saline of pH 7.4 was added to the different concentrations of mehani extract and ascorbic acid standard (50, 100, 150,200, 250 µg/ml). The absorbance was read at 230nm after 10 min of incubation. Hydrogen peroxide without extract was used as blank. The percentage of hydrogen peroxide scavenging activity was calculated using: % of hydrogen peroxide scavenging activity = $((A_C - A_S)/A_C) * 100$.

2.5.3 Nitric Oxide Scavenging Activity Assay

2ml of 10mM sodium nitroprusside prepared in phosphate-buffered saline (pH 7.4) was added to different concentrations (5 - 250µg/ml) of mehani extract and incubated at 30°C for 2h. Later, 0.5 mL was taken and added to 1.0 ml sulfanilic acid (33% in 20% glacial acetic acid) and incubated at room temperature for 5 min. 1.0 mL of 0.1ml naphthyl ethylenediamine dihydrochloride was added and incubated for 30 min (Lee 1992). The absorbance of the extract formed due to diazotization of nitrite when mixed with sulfanilic acid reagent and naphthyl ethylenediamine dihydrochloride was measured read at 550nm that can be calculated using $((A_C - A_S)/A_C) * 100$. A_C = absorbance of the control, A_S= absorbance of the sample.

2.5.4 Reducing Power Assay

Plant extracts that have reducing power activity on reacting with potassium ferric cyanide (Fe^{3+}) forms potassium ferrocyanide (Fe^{2+}) that further reacts with ferric chloride and forms ferric ferrous complex having an UV absorption at 700nm. Different concentrations of mehani extract were added to 2.5ml of potassium ferricyanide and kept in a water bath at 50°C for 20 minutes. Then, 2.5 ml trichloroacetic acid (10%) was added and centrifuged for 10 min at 3000 rpm. The supernatant was mixed with 0.5ml of freshly prepared ferric chloride solution and 2.5ml of distilled water. Then the absorbance was measured at 700 nm. Ascorbic acid was used as a standard (Oyaizu 1986).

2.6. Anti-Diaetic Assay

2.6.1 Alpha Amylase Inhibition Assay

It is important to block intestinal enzymes like α -amylase and α -glucosidase that break down the starch to simple glucose molecules and increases the postprandial glucose level. So the mehani extract will be evaluated for the inhibition of α -amylase enzyme. To the different concentrations of mehani NPs and ascorbic acid standard, 500 μl of α -amylase (0.5mg/ml) prepared in phosphate buffer (pH 6.9, 0.20 mM) was added and at 25°C for 10 min at 25°C. Then, 500 μl of 1 % starch solution prepared in sodium phosphate buffer (pH 6.9, 0.02 M) was added and again incubated at 25°C for 10

min. 1.0 ml of 3, 5 dinitrosalicylic (DNS) acid was then added and kept in a boiling water bath for 5 min that acts as a stopping reagent. The reaction mixture was cooled, and 10ml of distilled water was added, and absorbance was read at 540nm (KIM *et al.* 2000). The alpha-amylase inhibitory activity was expressed as a percentage of inhibition. Inhibition (%) = $[(A_c - A_s)/A_s] \times 10$. A_c =absorbance of the control; A_s = absorbance of the samples.

3. RESULTS & DISCUSSION

3.1. Alpha Amylase Inhibition Assay

Mehani acts as a reducing agent for the synthesis of AgNPs and FeNPs. The presences of phenols and flavonoids, and other secondary metabolites helps in synthesis of nanoparticles of different morphology (KSV 2017). The formation of brown and black color after mixing with extract is due to excitation of surface plasmon vibration. Absorbance peak near 450nm from UV-Vis spectra corresponds to the absorbance of synthesized AgNPs. Peaks were not obtained for iron nanoparticles as it is zero valent in nature. The FeNPs shows continuous absorption spectra without any strong peak conforms to the formation of zero-valent iron nanoparticles. The minor peaks at 216nm were due to the excitation of surface plasmon vibrations in the FeNPs solution, and these are identical to the characteristics UV-visible spectrum of metallic Iron. Figure 1 shows UV-Vis spec analysis of silver and iron nanoparticles.

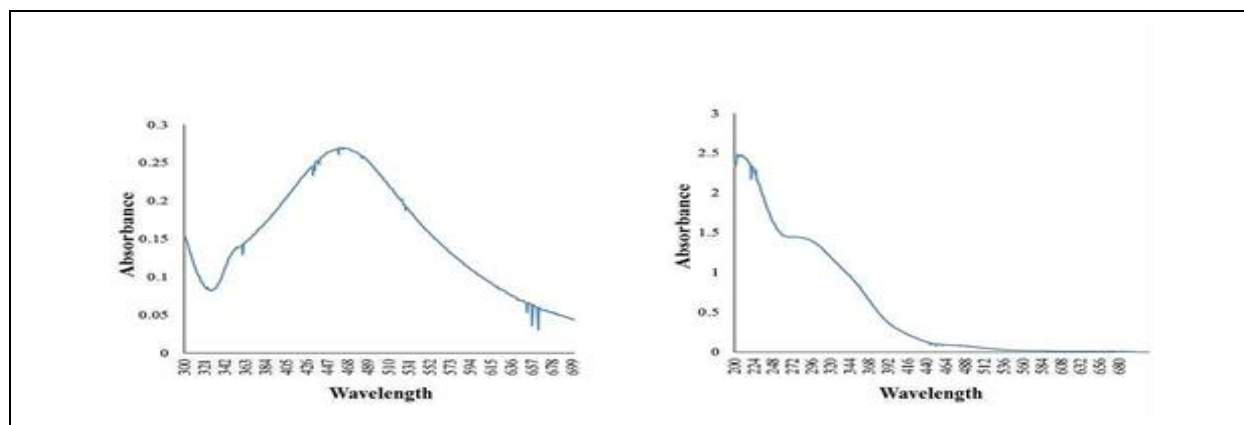


Fig. 1: UV Spec Analysis of AgNPs and FeNPs

3.2 FTIR Analysis

The possible biomolecules in the polyherbal formulation responsible for capping that cause reduction and stabilization of nanoparticles can be known using FTIR spectroscopy. Figure 2 displays the peaks observed in the extract, nanoparticles and the possible functional groups involved in the formation NPs. The bands at 1016 and 1020 cm^{-1} (C–OH stretching) are typical

polysaccharides. The bands at 1654 and 1535 cm^{-1} are characteristic of amide I and II bands. The band at 1454 cm^{-1} is assigned to the methylene group from the proteins that can bind to the silver nanoparticle through either free amine groups or residues in the proteins stabilizes silver nanoparticles (Sadeghi *et al.* 2015). The strong, broad peak at 3000–3600 cm^{-1} is characteristic of the N-H stretching vibration. Also, the hydroxyl peak at 3396 and 3468 cm^{-1} that decrease in the presence of nanoparticles,

indicating that Ag^+ ion is reduced with the hydroxyl groups of the flavonoid and polyphenol. The peak shifted from 3313 to 3457 cm^{-1} indicating that polyphenols are involved in the synthesis of iron nanoparticles. The peak at 1623 cm^{-1} revealing the involvement of $\text{C}=\text{O}$ stretching vibration of acid derivatives, and the weak band at 1018 cm^{-1} is attributed to amide groups. Peaks at 454 cm^{-1} indicates the characteristic band of metal ions. Certain peaks appeared in the FT-IR spectrum of extract alone that disappeared in FT-IR spectra of green synthesized Ag and FeNPs. This disappeared peak indicates the bioactive compounds from extracts, especially polyphenols, are involved in the reduction of silver and iron nanoparticles (K&J 2017).

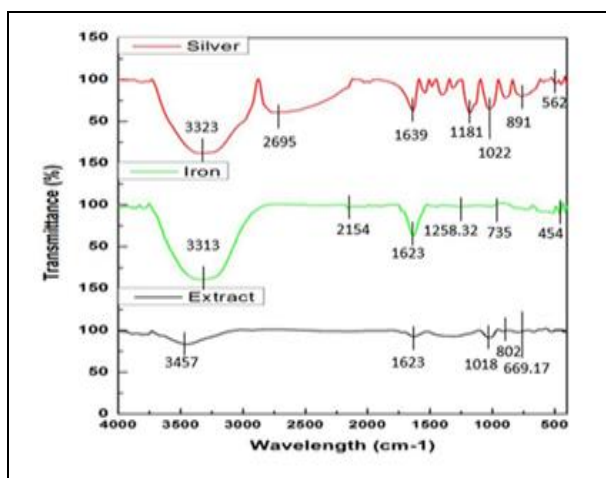


Fig. 2: FTIR Analysis

3.3 XRD Analysis

The synthesized NPs in figure 3 were highly crystalline with diffraction peaks assigned to the face-centred cubic phase of metallic iron. Figure 5 shows diffraction peaks are obtained at 38.1° , 44.08° , 64.2° , and 77.09° that are assigned to the (111), (200), (220), and (311) planes of a face centre cubic lattice of silver and iron were obtained. The intense diffraction peaks indexed to (220), (311), (400), (422), (511) and (440) planes appearing at $2\theta = 29.6^\circ$, 36.5° , 44.6° , 54.3° , 58.2° and 63.6° , respectively, coincide with the standard XRD data for silver and iron nanoparticles with a face-centered cubic structure. The crystallite size can be estimated by applying the scherres equation. These peaks were matched with the database of Joint Committee on Powder Diffraction Standards (JCPDS) file No. 89-3722, 75-0033, which indicates the crystalline nature of silver and iron nanoparticles.

3.4. SEM Analysis

Scanning Electron Microscopy (SEM) analysis was carried out to study the surface phenomenon of the synthesized NPs .Figure 4 shows that the NPs were spherical in shape with a smooth surface, and the average size was found to be in the range of 70-80nm and 40-60nm for silver and iron nanoparticles, respectively.

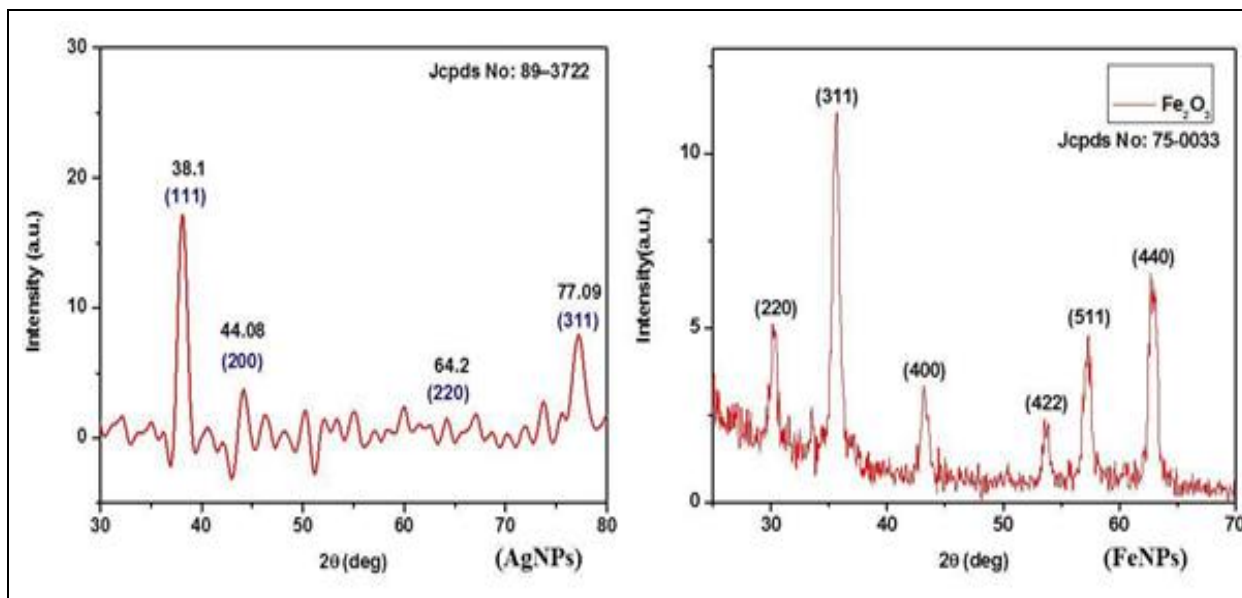


Fig. 3: XRD Analysis

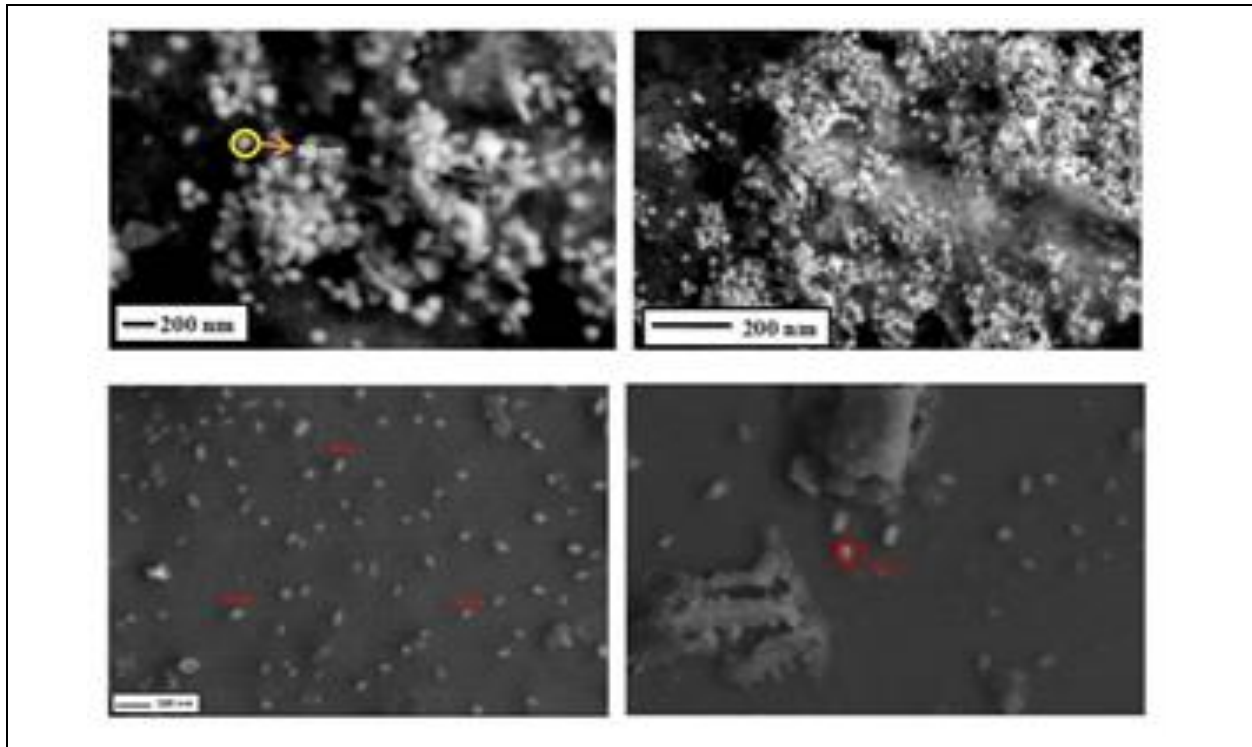


Fig. 4: SEM Analysis of Silver and Iron Nanoparticles

3.5 Determination of Total Phenolic Content

Total phenol content was estimated for NPs by Folin Ciocalteu's method using Gallic acid as standard. The reagent is formed from a mixture of phosphotungstic acid and phosphomolybdic acid, which after oxidation of the phenols, is reduced to a mixture of blue oxides of tungsten and molybdenum. The blue coloration produced has maximum absorption in the region of 750 nm and proportion to the total quantity of phenolic compound originally present. Total phenol was estimated for the synthesized nanoparticles and found to be 2.91 mg/gGallic acid Equivalent of AgNPs and 3.71 mg/gGallic acid Equivalent of FeNPs.

3.6 Determination of Total Flavonoid Content

The total flavonoid content for AgNPs and FeNPs was quantified by aluminum chloride colorimetric assay using rutin as standard as represented in figure 3. Aluminum chloride forms stable acid complexes with the C-4 keto groups and either the C-3 or C-5 hydroxide group of flavones and flavonols. The equation of standard curve is $y = 0.0014x + 0.0432$. The total flavonoid content was found to be 1.93 for mg/grutin equivalent of AgNPs, 5.185 mg/g rutin equivalent of FeNPs. The total phenol and figure.

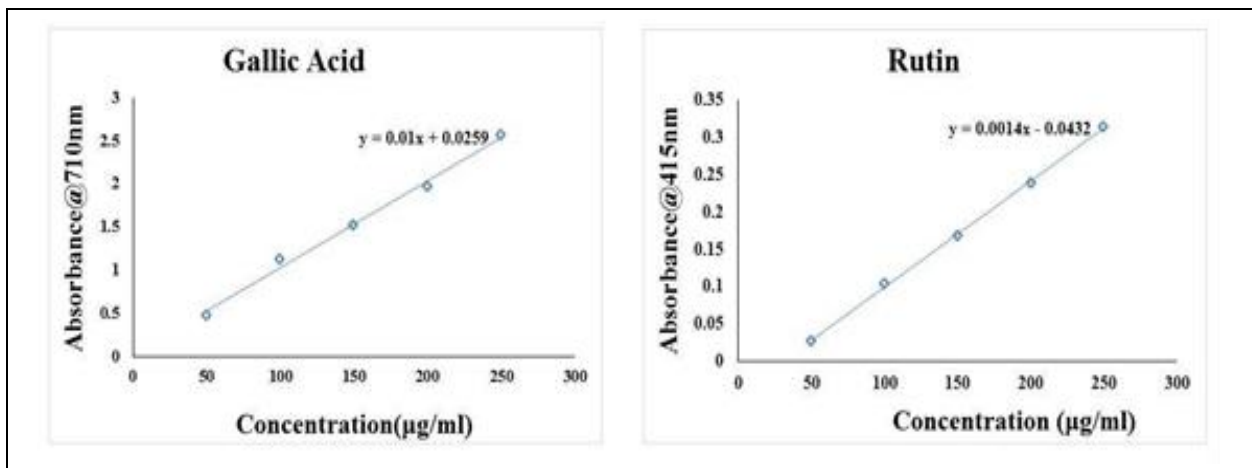


Fig. 5: Total Phenols and Flavonoids Content in AgNPs and FeNPs

3.7 DPPH Free Radical Scavenging Activity

The free radical scavenging activity of nanoparticles was determined for several concentrations of Ag and FeNPs (50-250 µg/ml) in figure 6 and compared with the standard ascorbic acid. Among the various concentration tested, the scavenging activity was found to be significant at 250 µg/ml. The highest percentage of 74.5% inhibition was found in FeNPs that is better than the standard ascorbic acid.

3.8 Nitric Oxide Scavenging Activity

The nitric oxide scavenging activity NPs was performed at varying concentrations (50-250 µg/ml) and compared with standard ascorbic acid. In Figure 7, FeNPs comparatively showed better activity than AgNPs with highest percentage of inhibition at 250µg/ml (62.65%). Ascorbic acid showed slightly higher activity of 71.11%.

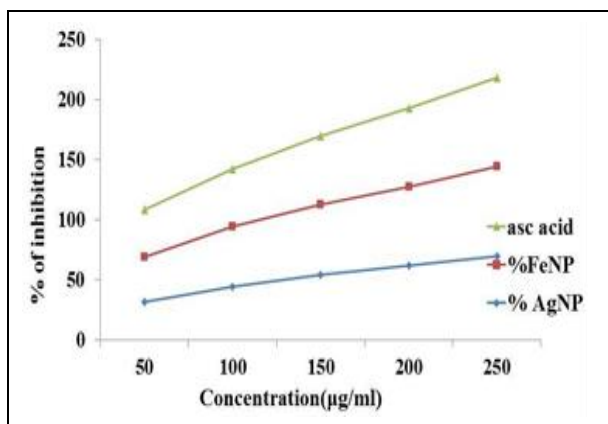


Fig. 6: DPPH Assay

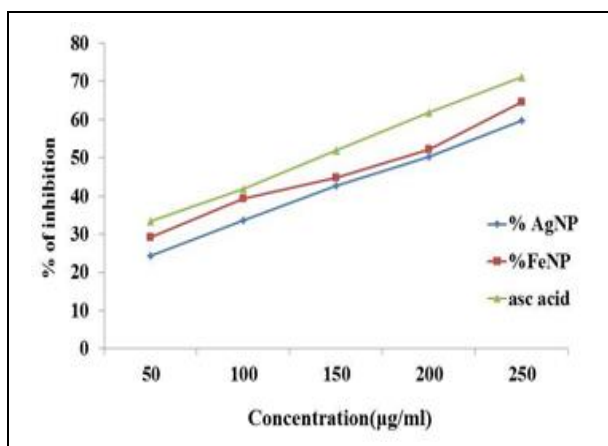


Fig. 7: Nitric Oxide Scavenging Activity

3.9 Hydrogen Peroxide Scavenging Activity

Different concentration (50-250µg/ml) nanoparticles were tested for Hydrogen peroxide scavenging activity and compared with standard ascorbic acid. Among these concentrations, the scavenging activity was significant at 250µg/ml, which is denoted in figure 8. The highest activity was found to 71.11 % (ascorbic acid), 64.75% (FeNPs), 58.6% (AgNPs) respectively.

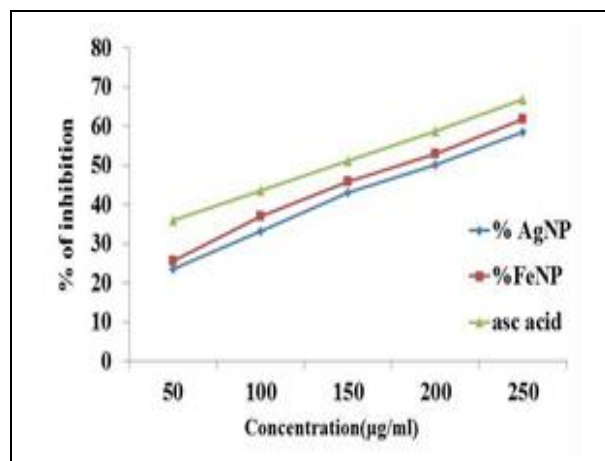


Fig. 8: Hydrogen Peroxide Scavenging Activity

3.10 Reducing Power Assay

Active compounds that can oxidize the intermediates produced during the lipid peroxidation process may act as strong oxidizing agents. The thereducing capabilities of AgNPS, FeNPs and standard ascorbic acid were found to be increasing with increasing concentrations (Chanda and Dave 2009). In figure 9, increased absorbance was found in ascorbic acid with 0.712 absorbances at 250µg/ml, 0.652 in FeNPs and comparatively lesser activity in AgNPs of 0.61 absorbances.

3.11 Anti-Diabetic Assay

3.11.1 α-Amylase Inhibition Activity

Different concentration of NPs and ascorbic acid was tested for α-amylase inhibitory effect by using starch as substrate. The result from figure 10 indicates that FeNPs shows significant and equivalent alpha-amylase enzyme inhibitory activity (70.48%) to the standard ascorbic acid (73.87%) at the maximum concentration of 250 µg/ml, indicating the usage mehani FeNPs for postprandial glucose control.

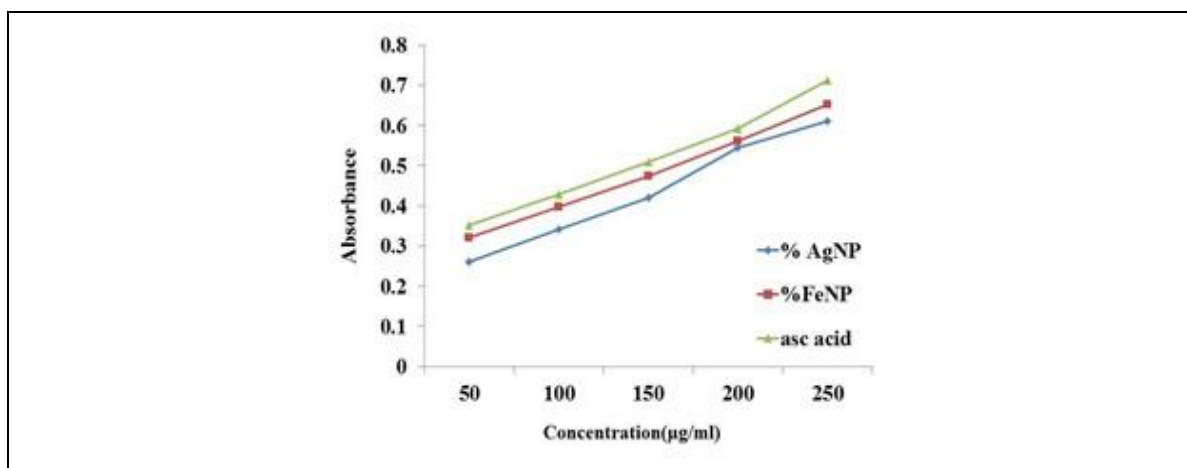


Fig. 9: Reducing Power Assay

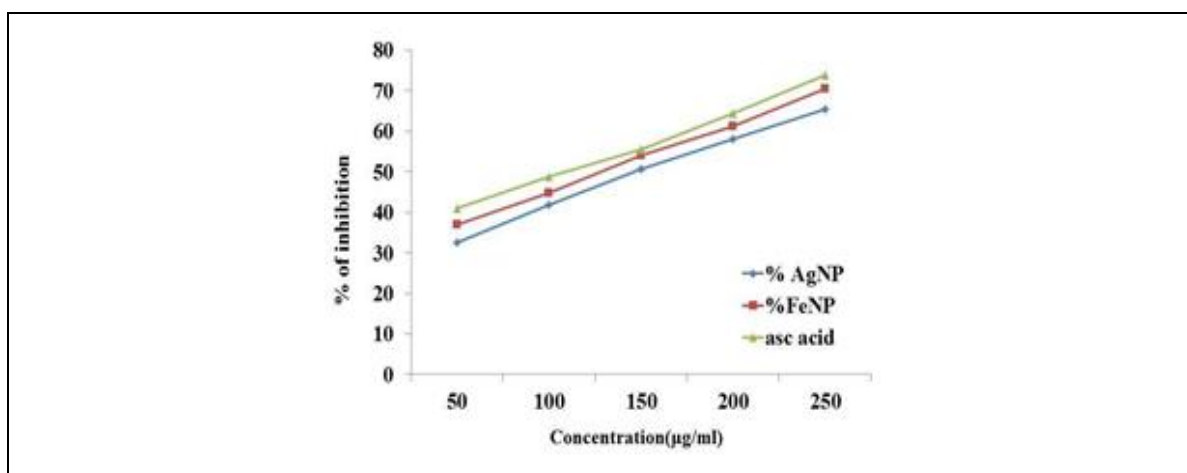


Fig. 10: α-Amylase Inhibition Activity

4. CONCLUSION

The silver and iron nanoparticles were synthesized using the polyherbal formulation through green synthesis that is an economical and eco-friendly methodology. Further, the characterization of synthesized nanoparticles was carried out using UV analysis, FTIR, XRD and SEM analysis. Initially, the UV analysis exhibited a strong peak at 465nm that confirms the formation of AgNPS. There was not any peak formation for FeNPs since it is zero valent in nature. FTIR analysis revealed the presence of bioactive compounds like phenols, flavonoids, polysaccharides that might be responsible for the reduction of nanoparticles. XRD analysis confirmed the presence of Ag and FeNPs by comparing them with standard JCPDS file No. 89-3722, 75-0033 and the peak indicated that the particles were highly crystalline in nature. The surface morphology and size of nanoparticles were analyzed by SEM, and it was found to be between 60-80nm and 40-60nm for AgNPS and FeNPS, respectively. Phenol and flavonoid content associated with the potent antioxidant property were estimated and found to be more for the

FeNPS when compared to the AgNPS. Antioxidant assays and anti-diabetic assay were performed to prospect the efficiency of nanoparticles synthesized from Mehani formulation, which could be used as a potent and alternate drug in treating diabetic complications with more efficacy and least side effects. The current study indicates that among the two nanoparticles synthesized using mehani, FeNPs possess more activity than AgNPs which could be properly utilized for nanoparticle based drug delivery. The antioxidant and anti-diabetic potential were also comparable with the standard drug. Further studies will help to completely validate the mechanism of action of mehani in alleviating diabetic complications and serve as an alternative to the current medications.

REFERENCES

- Bagherzade, G., Tavakoli, M. M., Namaei, M. H., Green synthesis of silver nanoparticles using aqueous extract of saffron (*Crocus sativus* L.) wastages and its antibacterial activity against six bacteria, *Asian Pac. J. Trop. Biomed.*, 7(3), 227–233 (2017).
<https://doi.org/10.1016/j.apjtb.2016.12.014>

- Balayssac, S., Trefi, S., Gilard, V., Malet-Martino, M., Martino, R., Delsuc, M.-A., 2D and 3D DOSY 1H NMR, a useful tool for analysis of complex mixtures: Application to herbal drugs or dietary supplements for erectile dysfunction, *J. Pharm. Biomed. Anal.*, 50(4), 602–612 (2009).
<https://doi.org/10.1016/j.jpba.2008.10.034>
- BLOIS, M. S., Antioxidant Determinations by the Use of a Stable Free Radical, *Nature*, 181(4617), 1199–1200 (1958).
<https://doi.org/10.1038/1811199a0>
- Chanda, S., Dave, R., In vitro models for antioxidant activity evaluation and some medicinal plants possessing antioxidant properties: An overview, *African J. Microbiol. Res.*, 3(13), 981–996 (2009).
<https://doi.org/10.1007/s13197-011-0276-5>
- Dewanjee, S., Das, A. K., Sahu, R., Gangopadhyay, M., Antidiabetic activity of Diospyros peregrina fruit: Effect on hyperglycemia, hyperlipidemia and augmented oxidative stress in experimental type 2 diabetes, *Food Chem. Toxicol.*, 47(10), 2679–2685 (2009).
<https://doi.org/10.1016/j.fct.2009.07.038>
- Giacco, F., Brownlee, M., Oxidative stress and diabetic complications., *Circ. Res.*, 107(9), 1058–70 (2010).
<https://doi.org/10.1161/CIRCRESAHA.110.223545>
- Jayaprakasha, G. K., Jaganmohan Rao, L., Sakariah, K. K., Antioxidant activities of flavidin in different in vitro model systems, *Bioorg. Med. Chem.*, 12(19), 5141–5146 (2004).
<https://doi.org/10.1016/j.bmc.2004.07.028>
- Kalia, A., Gauttam, V., Development of polyherbal antidiabetic formulation encapsulated in the phospholipids vesicle system, *J. Adv. Pharm. Technol. Res.*, 4(2), 108 (2013).
<https://doi.org/10.4103/2231-4040.111527>
- Kharisova, O. V., Dias, H. V. R., Kharisov, B. I., Pérez, B. O., Pérez, V. M. J., The greener synthesis of nanoparticles, *Trends Biotechnol.*, 31(4), 240–248 (2013).
<https://doi.org/10.1016/j.tibtech.2013.01.003>
- KIM, J.-S., KWON, C.-S., SON, K. H., Inhibition of Alpha-glucosidase and Amylase by Luteolin, a Flavonoid, *Biosci. Biotechnol. Biochem.*, 64(11), 2458–2461 (2000).
<https://doi.org/10.1271/bbb.64.2458>
- KSV, G., Green Synthesis of Iron Nanoparticles Using Green Tea leaves Extract, *J. Nanomedicine Biotherapeutic Discov.*, 7(1), 1-4 (2017)
<https://doi.org/10.4172/2155-983X.1000151>
- Lee, H. S., Antioxidative activity of browning reaction products isolated from storage-aged orange juice, *J. Agric. Food Chem.*, 40(4), 550–552 (1992).
<https://doi.org/10.1021/jf00016a004>
- Li, Z., Geng, Y.-N., Jiang, J.-D., Kong, W.-J., Antioxidant and Anti-Inflammatory Activities of Berberine in the Treatment of Diabetes Mellitus, Evidence-Based Complement. *Altern. Med.*, 1, 1–12 (2014).
<https://doi.org/10.1155/2014/289264>
- Lipinski, B., Pathophysiology of oxidative stress in diabetes mellitus., *J. Diabetes Complication,s* 15(4), 203–210 (2001).
[https://doi.org/10.1016/s1056-8727\(01\)00143-x](https://doi.org/10.1016/s1056-8727(01)00143-x)
- Liu, H., Liu, X., Jia, L., Liu, Y., Yang, H., Wang, G., Xie, L., Insulin therapy restores impaired function and expression of P-glycoprotein in blood-brain barrier of experimental diabetes., *Biochem. Pharmacol.*, 75(8), 1649–58 (2008).
<https://doi.org/10.1016/j.bcp.2008.01.004>
- McDonald, S., Prenzler, P. D., Antolovich, M., Robards, K., Phenolic content and antioxidant activity of olive extracts, *Food Chem.*, 73(1), 73–84 (2001).
[https://doi.org/10.1016/S0308-8146\(00\)00288-0](https://doi.org/10.1016/S0308-8146(00)00288-0)
- Nair, S. S., Kavrekar, V., Mishra, A., In vitro studies on alpha amylase and alpha glucosidase inhibitory activities of selected plant extracts, *Eur. J. Exp. Biol.*, 3(1), 128–132 (2013).
- Oyaizu, M., Studies on products of browning reaction. Antioxidative activities of products of browning reaction prepared from glucosamine., *Japanese J. Nutr. Diet.*, 44(6), 307–315 (1986).
<https://doi.org/10.5264/eiyogakuzashi.44.307>

- Patel, D., Prasad, S., Kumar, R., Hemalatha, S., An overview on antidiabetic medicinal plants having insulin mimetic property, *Asian Pac. J. Trop. Biomed.*, 2(4), 320–330 (2012).
[https://doi.org/10.1016/S2221-1691\(12\)60032-X](https://doi.org/10.1016/S2221-1691(12)60032-X)
- Sadeghi, B., Rostami, A., Momeni, S. S., Facile green synthesis of silver nanoparticles using seed aqueous extract of *Pistacia atlantica* and its antibacterial activity, *Spectrochim. Acta Part A, Mol. Biomol. Spectrosc.*, 134, 326–332 (2015).
<https://doi.org/10.1016/j.saa.2014.05.078>
- Zhishen, J., Mengcheng, T., Jianming, W., The determination of flavonoid contents in mulberry and their scavenging effects on superoxide radicals, *Food Chem.*, 64(4), 555–559 (1999).
[https://doi.org/10.1016/S0308-8146\(98\)00102-2](https://doi.org/10.1016/S0308-8146(98)00102-2)